Nonlinear Finite Element Analysis of Reinforced Concrete Beams Flexurally Strengthened with Carbon Fiber Reinforced Polymer Plates

Dr. Hassanien Mohammed Thiyab , lecturer , Kufa University
hasanein.alshammari@uokufa.edu.iq

Abstract: This study presents a three-dimensional nonlinear finite element model suitable for the analysis of reinforced concrete beams flexurally strengthened with CFRP (Carbon Fiber Reinforced Polymer) plates under static load using the ANSYS (Analysis SYStem) computer package. The eight-node iso-parametric brick elements are used to represent the concrete and the internal reinforcement may be modeled as an additional smeared stiffness distributed through concrete element in a specified orientation. Also, a membrane shell element which has four nodes with three translation degrees of freedom at each node has been used to model the CFRP plate. A Perfect bond is assumed between the elements. Material nonlinearities due to cracking, crushing of the concrete and yielding of the steel reinforcement are taken into consideration during the analysis. The behavior of concrete in compression is simulated by an elasto-plastic work hardening model followed by a perfect plastic response plateau which is terminated at the onset of crushing has been used .In tension, the crack is represented by a fixed smeared crack with post-cracking shear transfer model to simulate the aggregate interlock and dowel actions. The ANSYS computer program has been used to investigate the behavior of the different composite CFRP-reinforced concrete beams. The analytical results of load-deflection response along the examined beams have been compared with available experimental tests. In general, a good agreement between the finite element solutions and experimental results has been obtained with difference about (2 %). Parametric studies have been carried out to investigate the effect of some important material parameters. These parameters include the effect flexural strengthening method, thickness of CFRP, width of CFRP, longitudinal reinforcement and shear span length.

KEYWORDS : Finite Element; CFRP Plates; Nonlinear Analysis; Flexural Strengthening.

Introduction :

Concrete is a construction material with a high compressive strength and a poor tensile strength. A concrete structure without any form of reinforcement will crack and fail when subjected to a relatively small load. The failure occurs in most cases suddenly and in a brittle manner. To increase the structural load carrying capacity and ductility it needs to be reinforced. This is mostly done by reinforcing with steel bars that are placed in the structure before concrete is cast. The reinforcement then interacts with the hardened concrete so that the concrete and the steel together carry the load on the structure. Since a concrete structure usually has a long life the demands on the structure will normally change over time.In the extreme cases, a structure may be adverse and need to be repaired due to accidents (earthquake, explosions), change in loading, change in use and change in configuration. Another reason includes errors occur during the design or construction phase so that the structure needs to be strengthened before using it. To keep a structure at the same performance level it needs to be maintained at predestined time intervals. If the lack of maintenance has lowered the performance level of the structure, then the need for repairing it up to the original performance level may be required. In cases when higher performance levels are needed, upgrading is necessary. Where performance level means load carrying capacity, durability, function or aesthetic appearance. While upgrading refers to strengthening, increased durability, and change of function or improved aesthetic appearance. In this thesis, mainly strengthening is discussed. Today it exists many methods for strengthening a concrete structure, for example ; hand applied repairs with concrete mortar, shot concrete, injection techniques, different kind of concrete castings, (Carolin, 1999). However, an interesting strengthening method developed during the mid 70-ties was steel plate bonding. Even this method technically performs quite well, but it has some drawbacks. One is that the steel plates sometimes are quite heavy to mount at the work site. Another is the risk of corrosion at the joint between the steel and the adhesive. A third is that the joints between the steel plates must beform properly, which is based of the limited delivery lengths of the steel plates (Täljsten and Carolin, 1998). In recent years the development of the plate bonding repair technique has been shown to be applicable to many existing

strengthening problems in the building industry. This technique may be defined as one in which composite sheets or plates of relatively small thickness are bonded with an epoxy adhesive to, in most cases, a concrete structure to improve its structure behaviour and strength. The sheets or plates do not require much space and give a composite action between the adherents. The adhesive that is used to bond the fabric or the laminate to the concrete surface is a two-component epoxy adhesive, see Fig.(1).

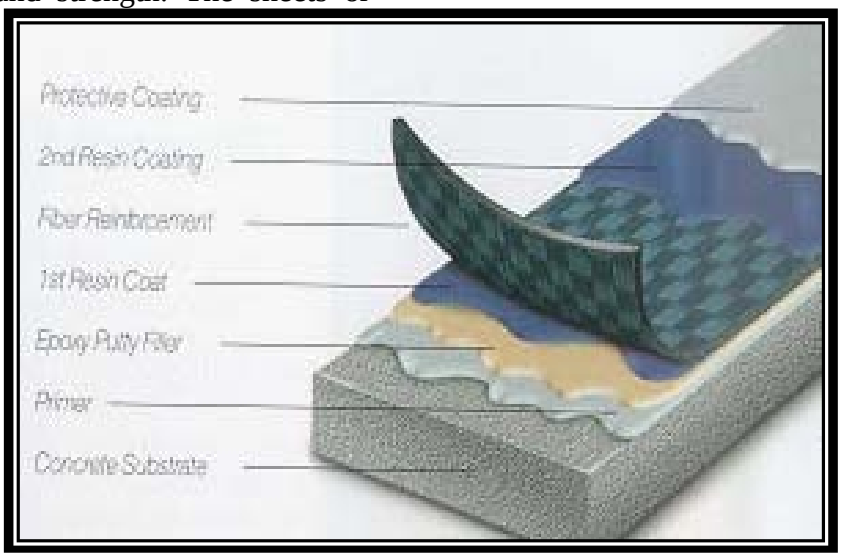

Fig.(1): Composite Strengthening System (Mbrace, 2001).

Finite element formulation for Concrete:

In the field of solid mechanics, the finite element is usually used to find approximate solutions for structures having complicated shapes and loading arrangement. In this study the concrete is represented by a hexahedron brick element having 8-nodes.The8-node isoparametric linear element shown in Fig. (2) is used in this study (DYANA, 1998). The element has eight corner nodes with three degrees of freedom u, v and w in the X, Y and Z direction respectively at each node.

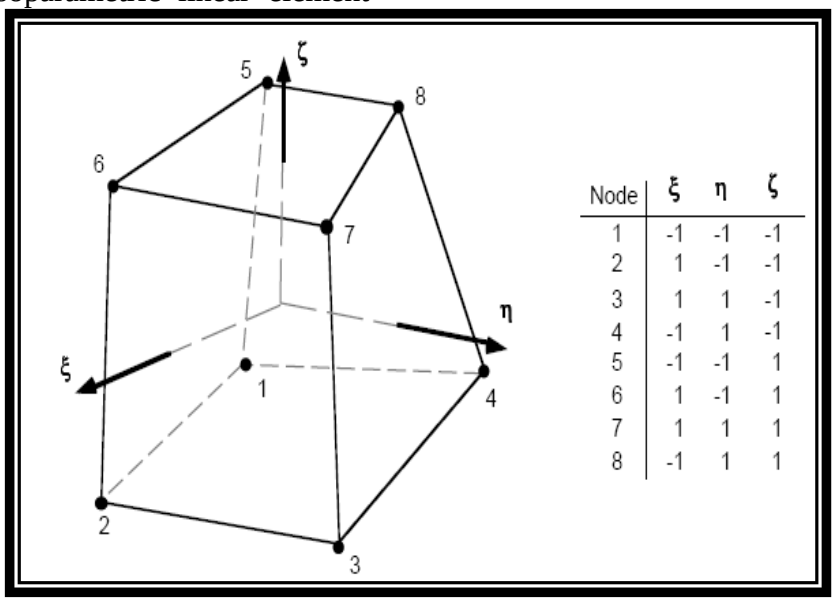

Node	ξ	η	ζ
1	-1	-1	-1
2	1	-1	-1
3	1	1	-1
4	-1	1	-1
5	-1	-1	1
6	1	-1	1
7	1	1	1
8	-1	1	1

Fig. (2): 8-Node Solid Hexahedron Element *(DYANA, 1998)*

Shape functions:

The shape functions for the 8- node brick element are introduced to express the coordinates and displacements of any point within the element in terms of nodal coordinates and displacements.

The local coordinates of the 8-node brick element are placed at the centre of the brick and are given in terms of ξ, η, ζ which range from - 1 to +1 as shown in Fig. (3). The isoparametric definition of the brick element is:

$$u(\xi,\eta,\zeta)=\sum_{i=1}^{8}N_i(\xi,\eta,\zeta).u_i$$

$$v(\xi,\eta,\zeta)=\sum_{i=1}^{8}N_i(\xi,\eta,\zeta).v_i \qquad \text{.....(1)}$$

$$w(\xi,\eta,\zeta)=\sum_{i=1}^{8}N_i(\xi,\eta,\zeta).w_i$$

Where N_i (ξ, η, ζ) is the shape function at the i-th node and u_i, v_i, w_i are the corresponding nodal displacements. The shape functions for the 8-node brick element which are adopted to map the element are given in Table 3.1.

Table (1): Shape Functions for the 8-Node Hexahedral Element (*Mottoram and Shaw,* 1996 and *Muhsen*, 2002)

LOCATION	ξ_i	η□	ζ_I	N_I (ξ_i, η_I, ζ_I)
Corners nodes	±1	±1	±1	$0.125(1+\xi\xi_i)(1+\eta\eta_i)(1+\zeta\zeta_i)$

Evaluation of Element Stiffness Matrix:

The function N_i is a function of local coordinates while the strains given in Eq. (2) are function of global coordinates. Therefore, a relationship between the derivatives in the two coordinate systems must be defined.

$$\{\varepsilon\}=\begin{Bmatrix}\varepsilon_x\\ \varepsilon_y\\ \varepsilon_z\\ \gamma_{xy}\\ \gamma_{yz}\\ \gamma_{zx}\end{Bmatrix}=\begin{Bmatrix}\frac{\partial u}{\partial x}\\ \frac{\partial v}{\partial y}\\ \frac{\partial w}{\partial z}\\ \frac{\partial u}{\partial x}+\frac{\partial v}{\partial y}\\ \frac{\partial v}{\partial y}+\frac{\partial w}{\partial z}\\ \frac{\partial w}{\partial z}+\frac{\partial u}{\partial x}\end{Bmatrix} \qquad \text{……. (2)}$$

The total derivatives of a typical shape function N_i are given as:

$$\begin{Bmatrix}\frac{\partial N_i}{\partial \xi}\\ \frac{\partial N_i}{\partial \eta}\\ \frac{\partial N_i}{\partial \zeta}\end{Bmatrix}=\begin{bmatrix}\frac{\partial x}{\partial \xi} & \frac{\partial y}{\partial \xi} & \frac{\partial z}{\partial \xi}\\ \frac{\partial x}{\partial \eta} & \frac{\partial y}{\partial \eta} & \frac{\partial z}{\partial \eta}\\ \frac{\partial x}{\partial \zeta} & \frac{\partial y}{\partial \zeta} & \frac{\partial z}{\partial \zeta}\end{bmatrix}\begin{Bmatrix}\frac{\partial N_i}{\partial x}\\ \frac{\partial N_i}{\partial y}\\ \frac{\partial N_i}{\partial z}\end{Bmatrix}=[J]\begin{Bmatrix}\frac{\partial N_i}{\partial x}\\ \frac{\partial N_i}{\partial y}\\ \frac{\partial N_i}{\partial z}\end{Bmatrix} \qquad \text{……. (3)}$$

Where, [J] is the Jacobian matrix of the global coordinates with respect to the local coordinates.

The global coordinates are expressed in terms of the local coordinates (by the same shape functions for displacements) as:

$$x=\sum_{i=1}^{8} N_i x_i \quad ; \quad y=\sum_{i=1}^{8} N_i y_i \quad ; \quad z=\sum_{i=1}^{8} N_i z_i \qquad \text{..... (4)}$$

Where: xi, y_i, and z_i, are the nodal coordinates.

By substitution of these relations in Eq.(3) , the Jacobian [J] is constructed in the following form:

$$[J]=\begin{bmatrix} \sum_{i=1}^{8} \frac{\partial Ni}{\partial \xi}.x_i & \sum_{i=1}^{8} \frac{\partial Ni}{\partial \xi}.y_i & \sum_{i=1}^{8} \frac{\partial Ni}{\partial \xi}.z_i \\ \sum_{i=1}^{8} \frac{\partial Ni}{\partial \eta}.x_i & \sum_{i=1}^{8} \frac{\partial Ni}{\partial \eta}.y_i & \sum_{i=1}^{8} \frac{\partial Ni}{\partial \eta}.z_i \\ \sum_{i=1}^{8} \frac{\partial Ni}{\partial \zeta}.x_i & \sum_{i=1}^{8} \frac{\partial Ni}{\partial \zeta}.y_i & \sum_{i=1}^{8} \frac{\partial Ni}{\partial \zeta}.z_i \end{bmatrix} \qquad \text{..... (5)}$$

Then the derivatives of the shape functions with respect to the global coordinates can be found by inverting [J], as:

$$\begin{Bmatrix} \frac{\partial N_i}{\partial x} \\ \frac{\partial N_i}{\partial y} \\ \frac{\partial N_i}{\partial z} \end{Bmatrix} = [J]^{-1} \begin{Bmatrix} \frac{\partial N_i}{\partial \xi} \\ \frac{\partial N_i}{\partial \eta} \\ \frac{\partial N_i}{\partial \zeta} \end{Bmatrix} \qquad \text{..... (6)}$$

The elemental volume in the global coordinates (dx, dy and dz) can be written in terms of local coordinates (dξ, dη, dζ) as

$$\mathbf{dV_e = dx\ dy\ dz = det[J] d\xi\ d\eta\ d\zeta} \qquad \text{.....(7)}$$

$$[K]=\sum_{n}[k]=\sum_{n}\int_{ve}[B]^T.[D].[B].dv_e \qquad \text{..... (8)}$$

Where: [*K*] is the stiffness matrix of the element assemblage and is given by

[*k*] is the element stiffness matrix.By substituting Eq (7) into (8), the element stiffness matrix may be written in the form

$$[K]^e = \int_{-1}^{+1}\int_{-1}^{+1}\int_{-1}^{+1} [B]^T [D][B]|J|d\xi d\eta d\zeta \qquad \text{..... (9)}$$

Fibre Reinforced Polymer (FRP) Representation:

The 4-node quadratic-order membrane shell element shown in Fig. (3) is used in the present work to model the FRP. This element has four corner nodes with three degrees of freedom u, v and w in the X, Y and Z direction respectively at each node.

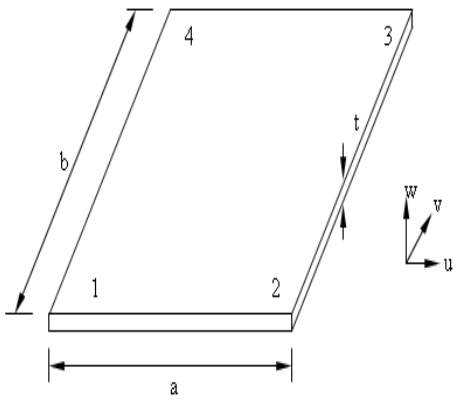

Fig. (3): Shell Element Geometry and Nodal

Shape Function & Evaluation of Stiffness Matrix:

The local coordinates of the 4-node shell element are placed at the center of the shell and are given in terms of ξ, η, ζ which range from - 1 to +1 as shown in Fig. (4). The isoparametric definition of the shell element is:

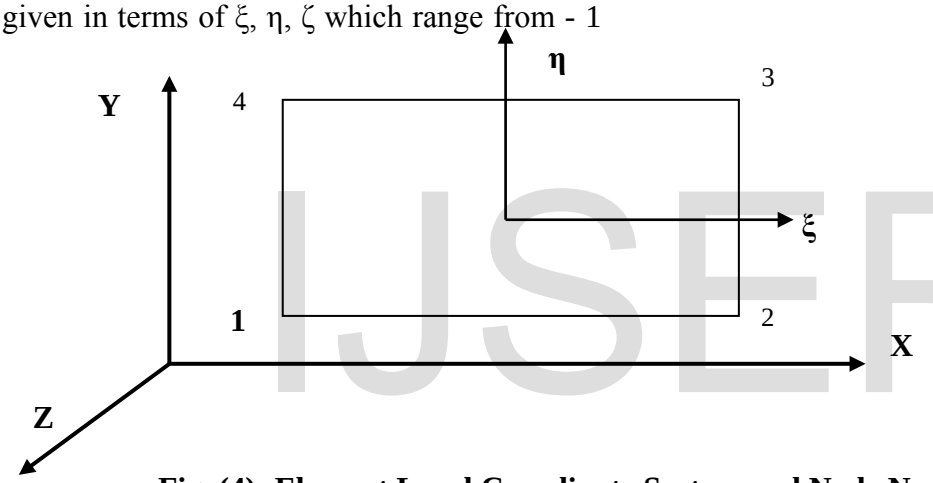

Fig. (4): Element Local Coordinate System and Node Numbering

$$u(\xi,\eta,\zeta)=\sum_{i=1}^{4} N_i(\xi,\eta,\zeta).u_i$$

$$v(\xi,\eta,\zeta)=\sum_{i=1}^{4} N_i(\xi,\eta,\zeta).v_i \qquad \text{……. (10)}$$

$$w(\xi,\eta,\zeta)=\sum_{i=1}^{4} N_i(\xi,\eta,\zeta).w_i$$

The shape functions are the follows:

$$N_1=\frac{1}{4}(1-\eta)(1-\xi)$$

$$N_2=\frac{1}{4}(1+\eta)(1-\xi)$$

$$N_3=\frac{1}{4}(1+\eta)(1+\xi) \qquad \text{…….. (11)}$$

$$N_4=\frac{1}{4}(1-\eta)(1+\xi)$$

The global coordinates of any point, within the element, in term of the natural coordinates are:

$$x = \sum_{i=1}^{4} N_i x_i$$
$$y = \sum_{i=1}^{4} N_i y_i \qquad \text{.....}$$
$$z = \sum_{i=1}^{4} N_i z_i$$

(12)

The strain-displacement relationship is as follows:

$$\begin{Bmatrix} \varepsilon_x \\ \varepsilon_y \\ \varepsilon_z \end{Bmatrix} = \begin{Bmatrix} \dfrac{\partial u}{\partial x} \\ \dfrac{\partial v}{\partial y} \\ \dfrac{\partial u}{\partial y} + \dfrac{\partial v}{\partial x} \end{Bmatrix} \qquad \text{..... (13)}$$

The development of the stiffness characteristic of the shell element follows essentially the same procedure as that for the brick element, i. e.

$$[k]^e = \int_{-1}^{+1}\int_{-1}^{+1} [B]^T [D][B] |J| . d\xi . d\eta \qquad \text{..... (14)}$$

Reinforcement Idealization

In developing a finite element model for reinforced concrete members, at least three alternative representations of reinforcement have been used:

a) Discrete Representation.
b) Distribution Representation.
c) Embedded Representation.

This study adopted the distribution (smeared) representation which is shown in Fig.(5), the steel is assumed to be distributed in the concrete element with a particular orientation angleθ. In the composite concrete, reinforcement constitutive relation is used in this case [*ASCE (1981); Chen (1982*)]. To derive such a relation, perfect bond is usually assumed between the concrete and steel. In Ansys programme SOLID 65 allows the presence of four different materials within each element; one matrix (e.g. concrete) and a maximum of three independent reinforcing materials. The concrete material is capable of directional integration point cracking and crushing besides incorporating plastic and creep behaviour. The reinforcement (which also incorporates creep and plasticity) has uniaxial stiffness only and is assumed to be smeared throughout the element. Directional orientation is accomplished through user specified angles.

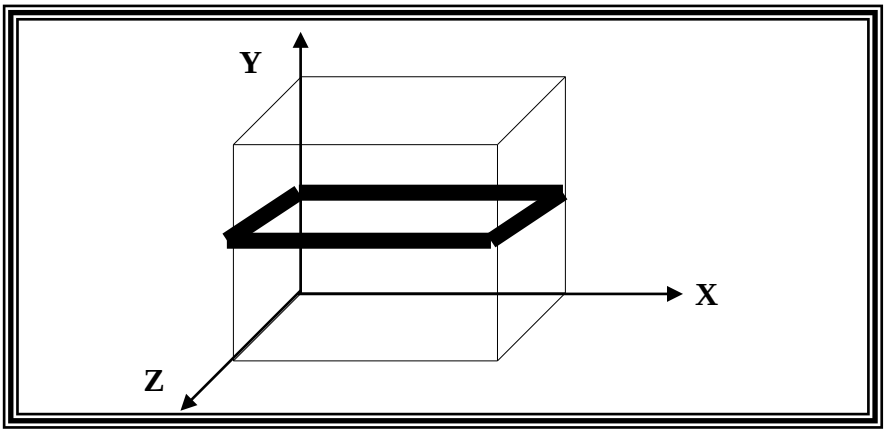

Fig. (5): Representation of distributed reinforcement

Zarnic et al. CFRP-Concrete Beam

A simply supported beam under four-point load tested by (Zarnic et al., 1999) was selected for the analysis using the proposed finite element models implemented in ANSYS computer program. Fig.(10) shows the specimen geometry and loading setup used for Zarnic et al. composite CFRP-concrete beam. The length of the simply concrete beam and CFRP plate was (2900 mm, 2800mm) respectively. The specimen had a rectangular concrete beam width of (200 mm) and a depth of (300 mm). Also, this specimen had CFRP plate which had a width of (50 mm) and a thick of (1.2 mm). External loading consisted of two point loads applied to the specimen at distance (960 mm) from each end.

Finite Element Idealization and Material Properties

As an advantage of symmetrical loading and geometry, only one-quarter of the beam has been used in the finite element analysis. The selected quarter was modeled using 104 elements, 90 of which are quadratic hexahedral brick elements and the other 14 are 4-node shell elements. The elements used to model the concrete beam were 8-quadratic brick elements. The CFRP plate was modeled using membrane shell elements, which had four nodes with three degrees of freedom at each node. They were attached to the nodes on the bottom surface of concrete beam. The finite element mesh, boundary and symmetry conditions and loading arrangement are shown in Fig.(11).

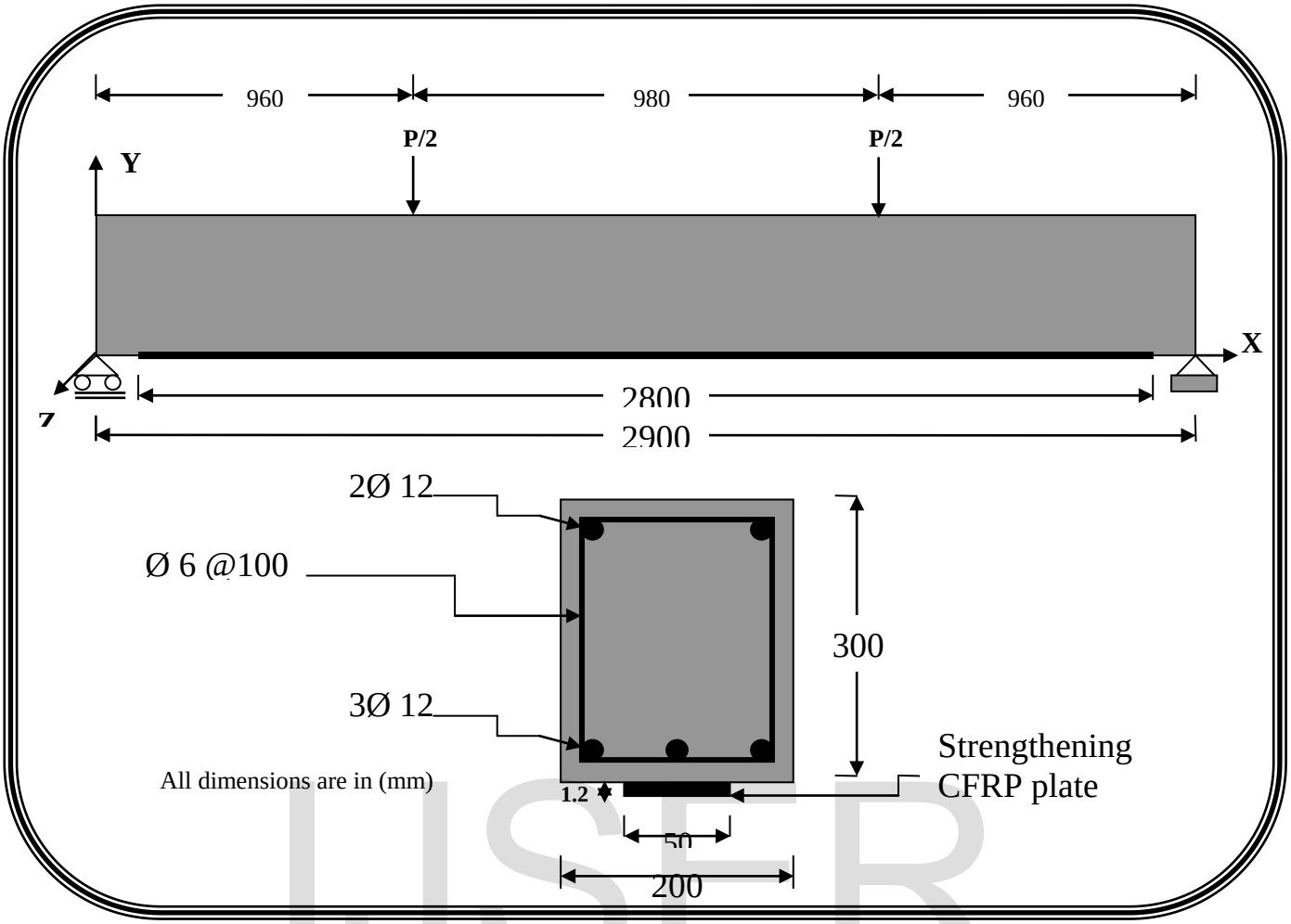

Fig.(10): Details of Zarnic et al. CFRP plated beam.

1450

All dimensions are in (mm)

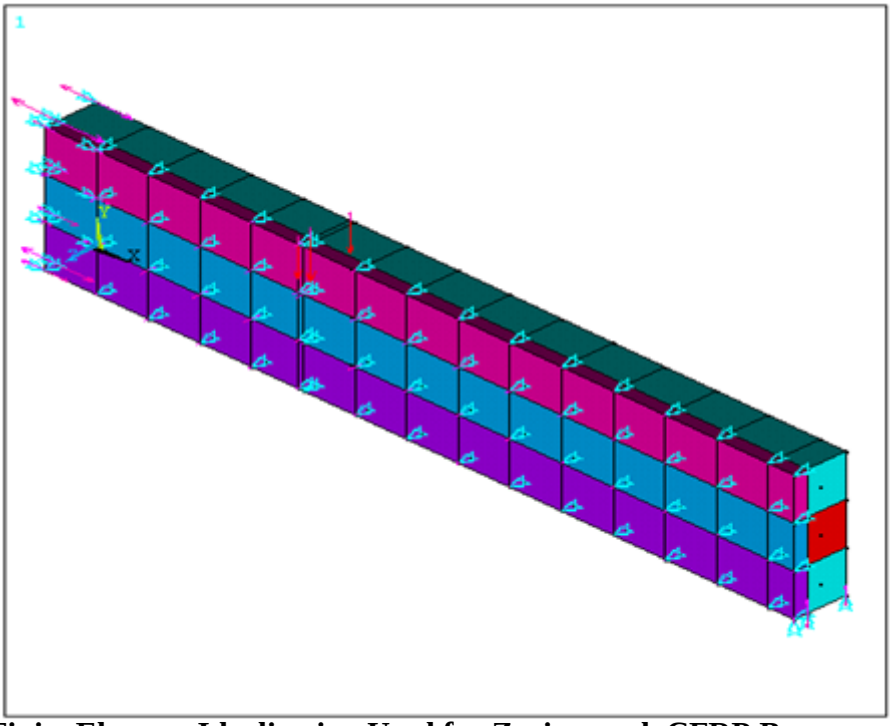

Fig.(11): Finite Element Idealization Used for Zarinc et al. CFRP Beam.

The external force and corresponding reaction were modeled as line loads uniformly distributed across the width of the beam. The main and shear reinforcement were modeled distribution (smeared) representation in the brick (concrete) elements. The material properties and the additional material parameters adopted in the analysis are given in Table (3). The 8-point rule, with a convergence tolerance of 0.1%, has been generally used to carry out the finite element analyses.

Table (3): Material Properties and Parameters Used for Zarinc et al. CFRP Plate Beam.

	Material properties and material parameter	Symbol	Value
Concrete	*Young's modulus*	Ec (N/mm^2)	27000
	Compressive strength	f'c (N/mm^2)	25
	Tensile strength	f_t (N/mm^2)	3.5
	Poisson's ratio	υ_c *	0.2
	Shear Transfer Coefficients	*Shr-Op**	0.2
		*Shr-Cl**	0.85
	Ultimate Biaxial Compressive Strength	f_{cb} (N/mm^2)	1.2 f'c
	Hydrostatic Stress	σ_h (N/mm^2)	1.507 f'c
	Ultimate Compressive Strength for a State of Biaxial Compressive	F_1 (N/mm^2)	1.45 f'c

	Superimposed on σ_h		
	Ultimate Compressive Strength for a State of Biaxial Compressive Superimposed on σ_h	F_2 (N/mm ^{2})	1.725 f'c
CFRP	*Young's modulus*	E_{CFRP}(N/mm^2)	150000
	Tensile strength	f_t (N/mm^2)	2400
	Poisson's ratio	ν_{CFRP} *	0.33
Steel	*Young's modulus*	E_s (N/mm^2)	210000
	Yield stress	f_y (N/mm^2)	460
	Poisson's ratio	ν_s	0.3

Results of Analysis

This section presents the finite element results obtained for Zarinc et al. CFRP plated concrete beam compared with the experimental results. The experimental and analytical load-deflection curves are shown in Fig.(1 2). Good agreement is obtained between the predicted finite element and the experimental load-deflection curves throughout the entire range of behavior of the tested specimen assuming perfect bond between concrete beam and CFRP plate. The computed ultimate load was slightly higher than the experimental ultimate load. The analytical ultimate load level (115 kN) is detected quite well compared with that experimentally observed (115.2 kN), with an error of only 0. 2 %.

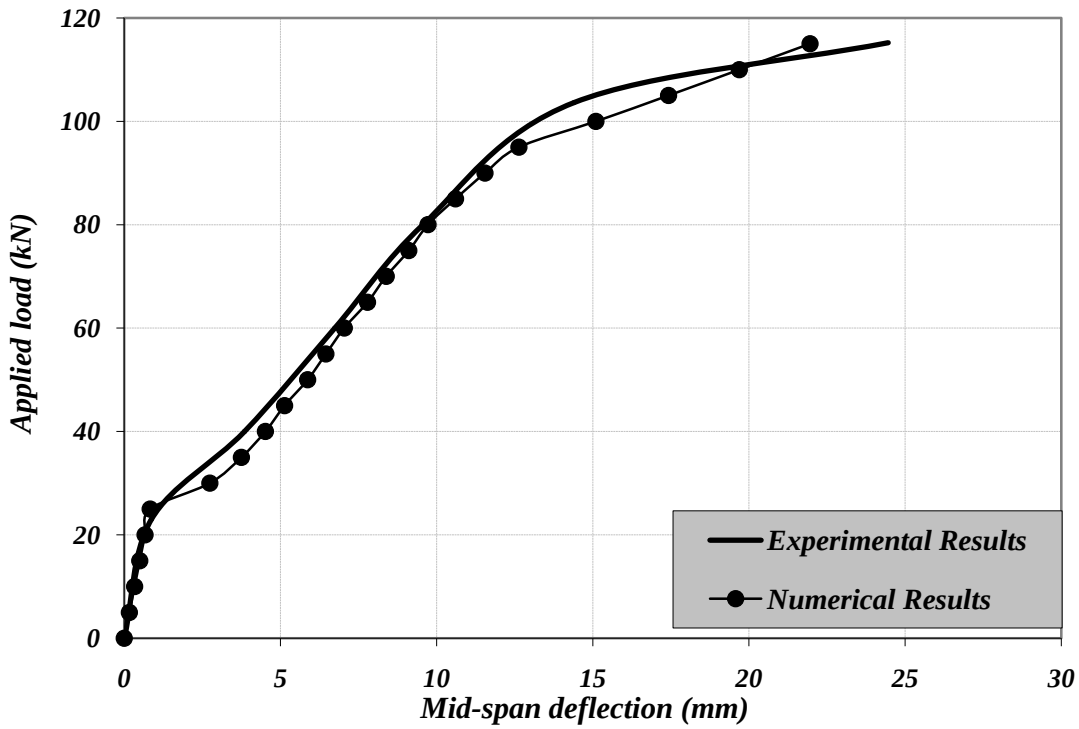

Fig.(1 2): Zarnic et al. CFRP Plated Concrete Beam , Experimental and Analytical Load-

Fig.(13) illustrate the numerical results for deform and un deform Zarinc et al. beam deflection in Y-direction

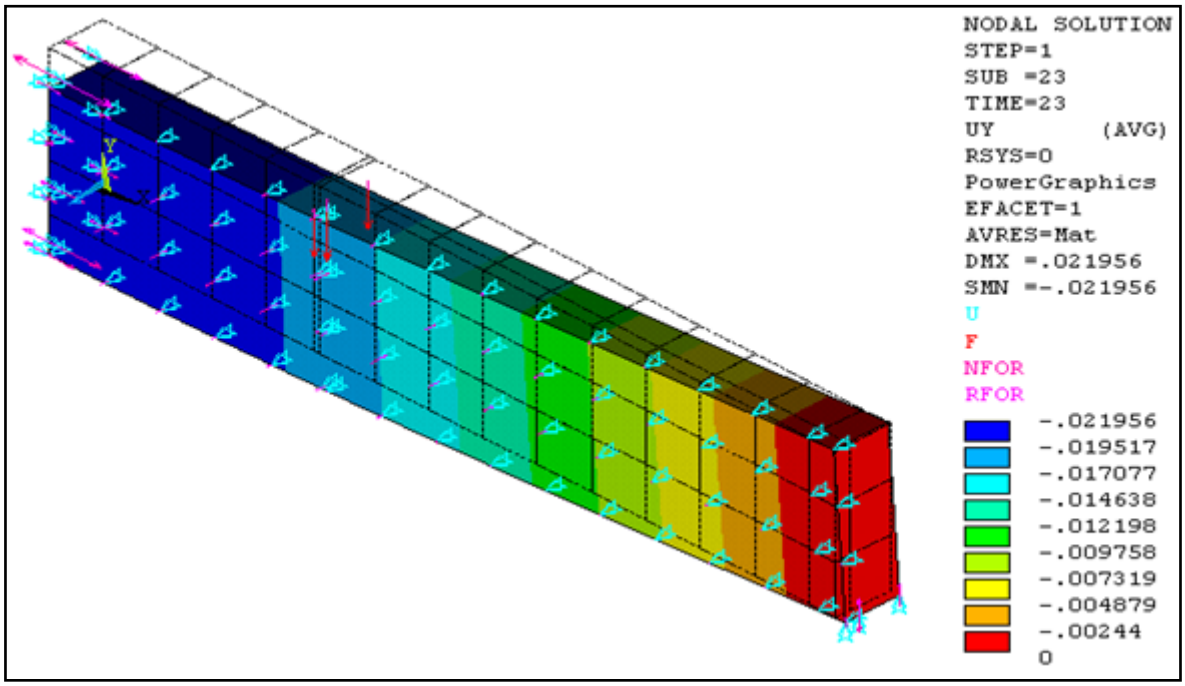

Fig.(13) : Zarnic et al, Deflection in Y-Direction,

Effect of method of Strengthening with CFRP Plate

In order to study the effect of method of strengthening with CFRP plate on the over all behavior of the concrete beam , Zarnic et al. beam has been analyzed for two cases (with CFRP and without CFRP). Fig.(13) shows the effect of method of strengthening of CFRP plate on the load-deflection response of reinforcement concrete beam for Zarnic et al. These figure show 30.6% increase in the ultimate load with CFRP for Zarnic et al. beam. From figure we can conclude that the method of strengthening with CFRP plate is very effective.

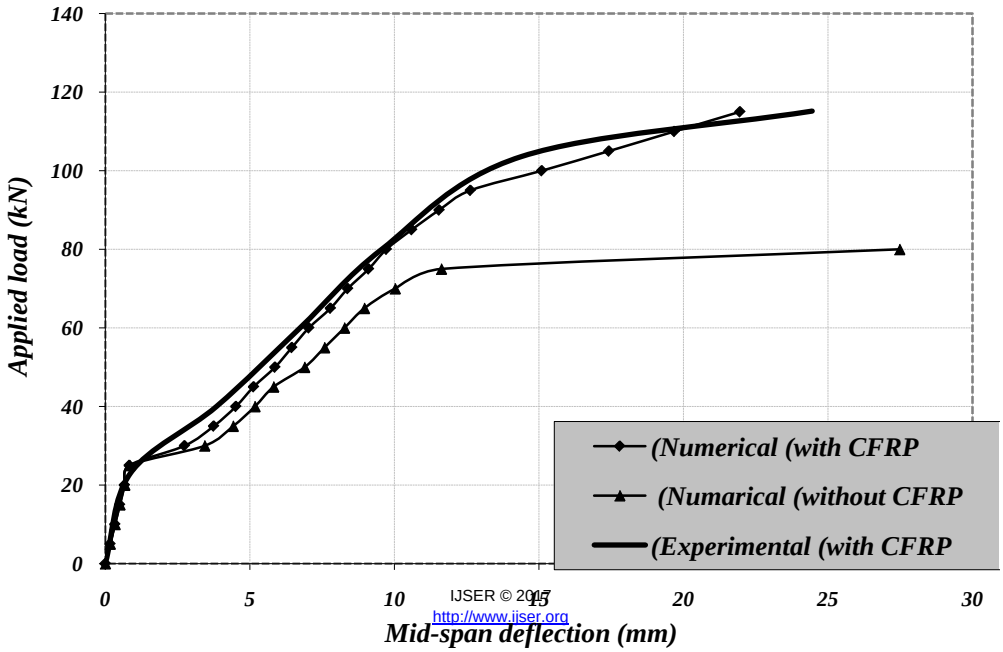

Fig.(13): Effect of Method of Strengthening with CFRP Plate on the Load-Deflection Behavior for Zarnic et al. concrete Beam

Effect of CFRP Plate Thickness

To study the effect of the thickness of the CFRP plate of the beam on the behavior of composite CFRP-concrete beam, different values CFRP thicknesses were considered. Zarnic et al. composite beam has been analyzed for different values of CFRP thickness. These values used in the finite element analysis were 0.5, 1, 1.5, 2 and 3 times thickness of CFRP plate in the experimental work and equal to 0.6 mm, 1.2 mm, 1.8 mm, 2.4 mm, 3.6 mm respectively. Fig.(14) shows the effect of CFRP thickness on the load-deflection behavior of the selected beam. This figure shows that increasing the CFRP thickness has a significant effect by increasing the ultimate load of the beam with decrease in deflection.

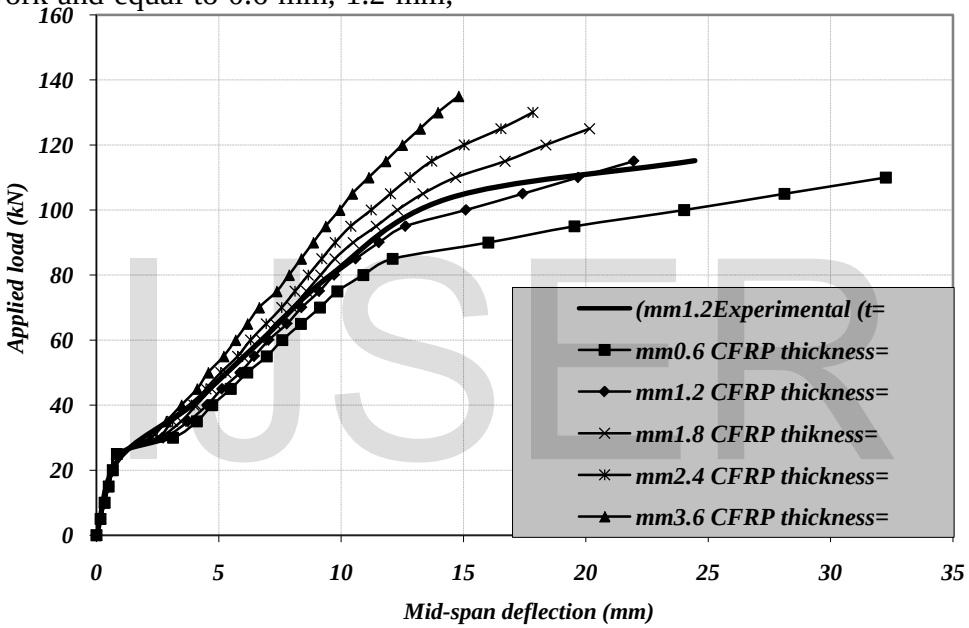

Fig.(14): Effet of CFRP Plate thickness on the Load-Deflection Behavior for Zarnic et al.

Effect of CFRP Plate Width

In order to investigate the effect of the CFRP plate width on the behavior of CFRP-concrete beam, Zarnic et al. beam analyzed with different values of CFRP width. These values used in finite element analysis were 50 mm, 100 mm, and 200 mm respectively. Fig.(15) shows the effect of CFRP plate width on the load-deflection response of CFRP-concrete beam. Generally, the CFRP width has a significant effect on the behavior of the composite beam.

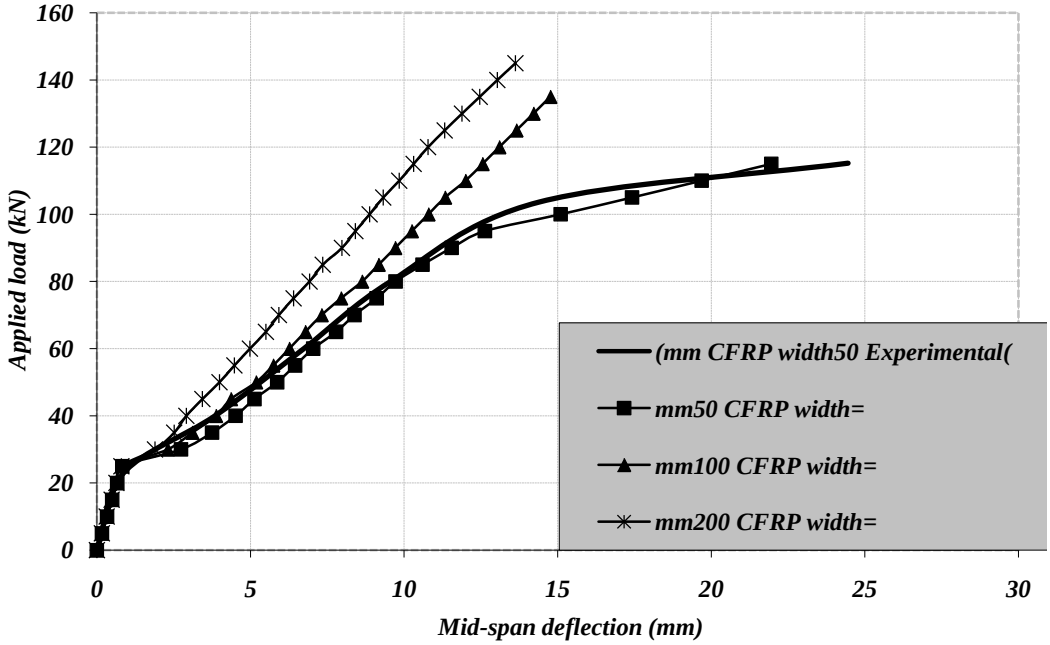

Fig.(15):Effect of CFRP Plate on the Load-Deflection Behavior for Zarnic et al. Beam

Effect of Depth of Beam

The effect of increasing the total depth (h) on the load-deflection response and the ultimate load was investigated. In this section the total depth (h) was increased from (300 mm) to (400 mm), (500 mm) and (600 mm). The result of this study leads to the conclusion that increasing the total depth has a significant role on load-deflection and ultimate load of composite CFRP-concrete beam. Fig.(16) shows the influence of total depth (h) increasing on the load-deflection response for the composite beam. This figure reveals that both initial and post cracking stiffness and the ultimate load are significantly increased as the total depth increased. This can be attributed to the fact that when the total depth is increased, the internal lever arm between the compression force in the concrete and the tensile force in tension reinforcement is significantly increased.

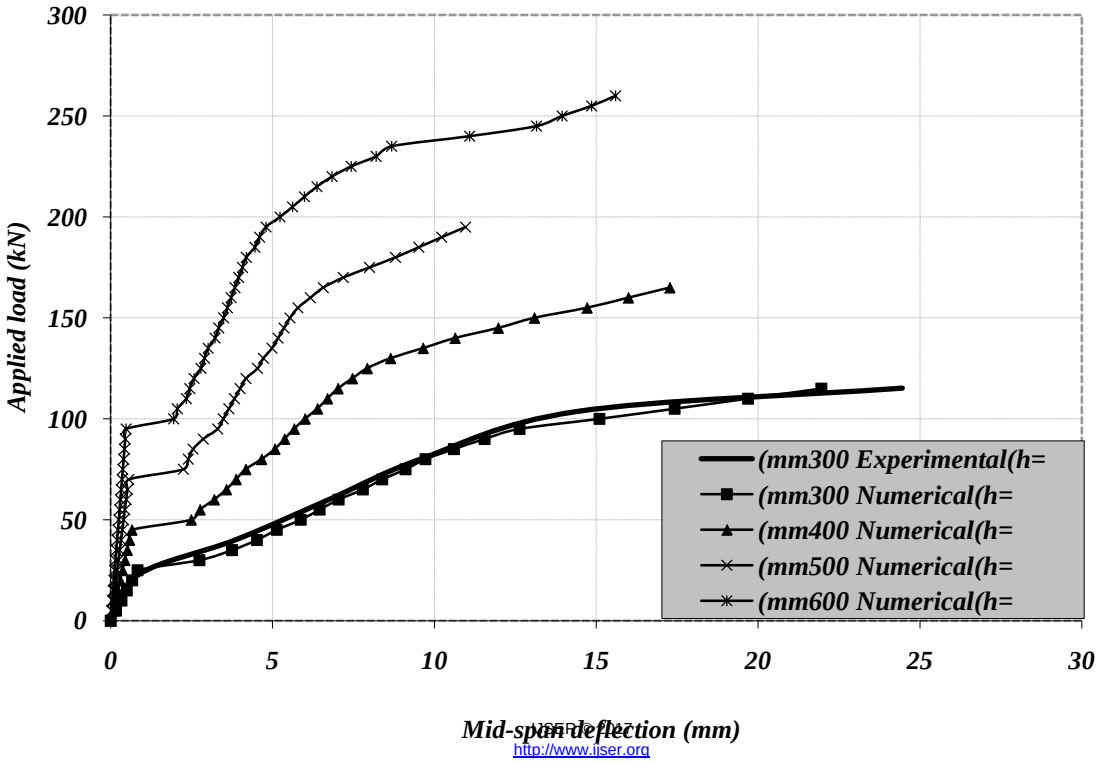

Fig.(16): Effect of Depth on Load-Deflection Behavior of Zarnic et al. Composite Beam

Effect of Length of Shear Span

In order to study the effect of the length of the shear span of the beam, five beams with different lengths of shear span (750 mm, 850 mm, 960 mm and 1050 mm) were analyzed numerically. Fig.(1 7) shows the load-deflection curves of the five shear span lengths of Zarnic et al. composite beam. This figure indicates that the increase in shear span decreases the ultimate load and increases the deflection of the beam for constant reinforcement ratio and vice versa. For different reinforcement ratios the increase of the shear span makes the increase of the reinforcement ratio to have a slight effect on the increasing of the ultimate load while the decrease of the shear span makes the increase of the reinforcement ratio to have a good effect in increasing the ultimate load.

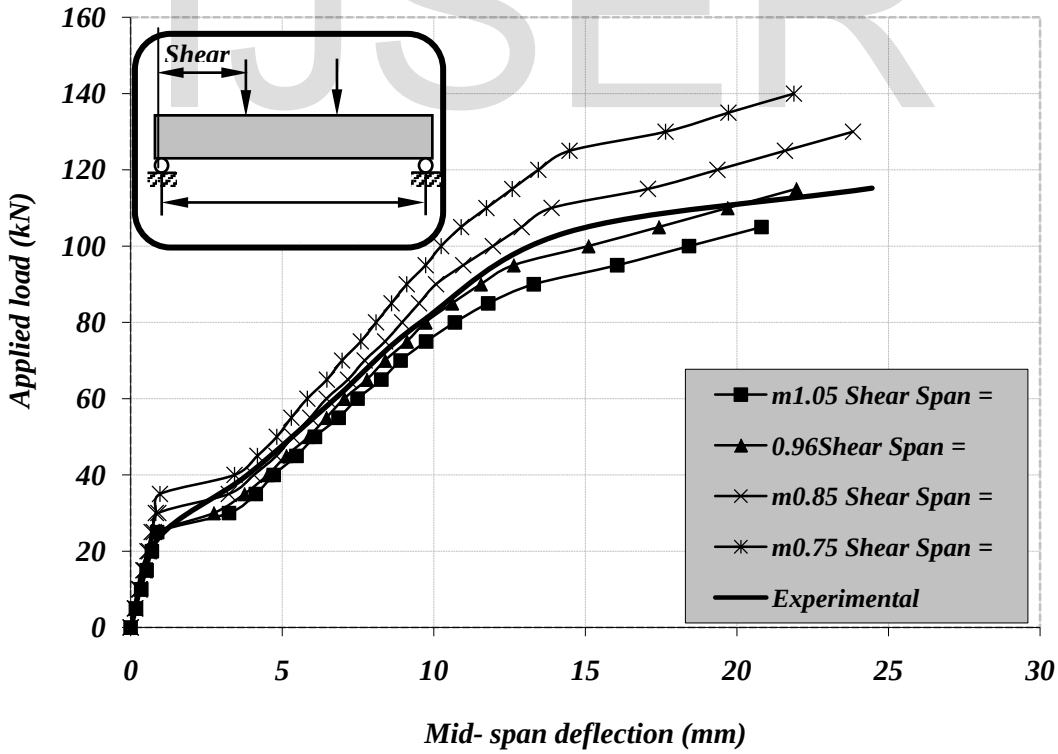

Fig.(1 7):Effect of Length of Shear Span on The Load-Deflection Curve for Zarnic et al. Composite

Effect of Longitudinal Reinforcement

In order to study the influence of longitudinal reinforcement on the behavior and ultimate load of the tested beam, different values of reinforcement area have been considered. The selected values were 0.5, 0.75, 1.0, 1.5 and 2 times the magnitude of the reinforcement area used in the experimental work, which was 565 mm^2. In this analysis the compressive strength and the shear span were kept constant.Fig. (18) shows that the magnitude of the reinforcement ratio affects the load-deflection curve and the ultimate load.

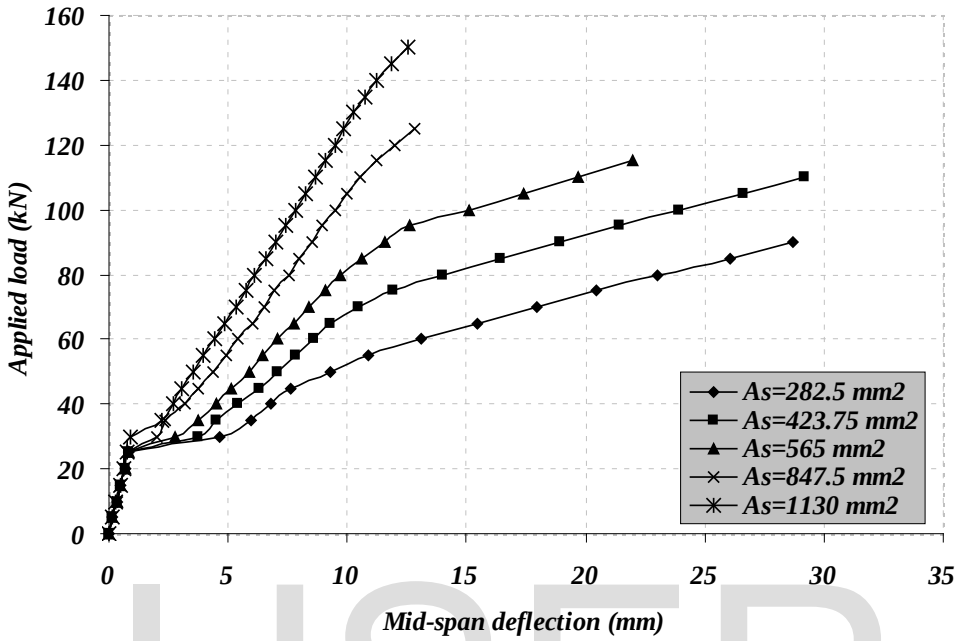

Fig.(18): Effect of Longitudinal Reinforcement Ratio on the Load-Deflection Behavior for Zarnic

Conclusions :

The results obtained from the present finite element method show that the computational models adopted in this study with ANSYS package technique are suitable for prediction of overall behavior of reinforced concrete beam strengthened with CFRP plate under static loading. The comparison between the numerical and the available experimental results has shown a good agreement with a difference of about (2%) respect to ultimate load.

1. The flexural strengthening of R.C. beams with CFRP is effective with increment in ultimate load of about (30-45) %.
2. The parametric study with respect to the thickness of the CFRP plate shows that this effect has a significant effect on the load–deflection behavior of CFRP-reinforced concrete beam. A 50%, 100% and 200% increase in the thickness of CFRP plate caused an increase of 9%, 13% and 17.2% in the ultimate load capacity of a specified CFRP-reinforced concrete beam respectively for Zarnic et al composite beam.
3. The width of the CFRP plate affects the overall load-deflection behavior of the CFRP-concrete beams. A 100% and 300% increase in the CFRP plate width caused an increase of 17 % and 26 % in the ultimate load capacity of the CFRP-reinforced concrete beam respectively for Zarnic et al composite beam.
4. The numerical analysis indicated that the ultimate load increases with the increase of the depth of the composite beam. It was noted that a 33%, 67%and 100% increase caused an increase 43%, 69% and 126% in the ultimate load capacity of the composite beam for Zarnic et al composite beam.
5. The shear span length affects the overall load-deflection behavior of the CFRP-concrete beam. As the shear span length of the

composite beam decreases, the ultimate load capacity increases. A 22%, 11% decrease and 9% increase of the shear span length caused an increase 39%, 13% and decrease 9% in the ultimate load capacity of the composite beam respectively for Zarnic et al composite beam.

6. A good increase in ultimate load is obtained from increasing the longitudinal reinforcement of the CFRP-concrete beam to (1.5-2) times the amount of reinforcement provided in the experimental work. The increase varied from (9 to 30 %) for Zarnic et al composite beam.

Refernces:

ANSYS, ***"ANSYS user's manual revision 5.4"*** ANSYS, Inc., Canonsburg, Pennsylvania, 1998

ASCE Committee on Concrete and Masonry Structures, "***A state of the art report on the finite element analysis of reinforced concrete***", , 1981.

Chen, W.F., "***Plasticity in reinforced concrete***", Third Edition, Mc Graw-Hill Company, New York. U.S.A., 1982.

Dawe, D.J., ***"Matrix and finite element displacement analysis of structures"***, , Oxfored, 1984.

Dyana, LS., ***"Theoretical manual"***, Technical Report, Livermore Software, Technology Corporation, 1998, pp.498.

Mbrace, "***Composite strengthening system with carbon fiber reinforcement***", Master Binders, 2001.

Mottoram, T.J., and Shaw, C.T. "***Using finite element in mechanical design***", McGraw-Hill Book CO., International, London, England, 1996.

Muhsen , H.N., ***"Three-dimensional nonlinear finite element analysis of axially loaded concrete-filled steel tube short columns",*** Master Thesis, University of Technology, Iraq, 2002.

Täljsten, B. and Carolin, A. ***"Strengthening of a concrete railway bridge in Luleä with carbon fiber reinforced polymers-CFRP"***, Technical Report, Luleä University of Technology, Sweden, 1998, pp.

Zarinc, R., Gostic, S., Bosiljikov, V. and Bokan-Bosiljikov, V., ***"Improvement of bending load-bearing capacity by externally bonded plates",*** ,1999, pp. 433-442.

Zienkiweicz, O.C., ***"The finite element method"***, Third Edition, Mc Graw. Hill, London, 1977.